HHS Public Access

Author manuscript

J Vis Exp. Author manuscript; available in PMC 2022 June 28.

Imaging Mitochondrial Ca^{2+} Uptake in Astrocytes and Neurons using Genetically Encoded Ca^{2+} Indicators (GECIs)

Nannan Zhang[1],

Zhe Zhang[1,2],

Ilker Ozden[2],

Shinghua Ding[1,2]

[1]Dalton Cardiovascular Research Center, University of Missouri-Columbia

[2]Department of Biomedical, Biological and Chemical Engineering, University of Missouri-Columbia

Abstract

Mitochondrial Ca^{2+} plays a critical role in controlling cytosolic Ca^{2+} buffering, energy metabolism, and cellular signal transduction. Overloading of mitochondrial Ca^{2+} contributes to various pathological conditions, including neurodegeneration and apoptotic cell death in various neurological diseases. Here we present a cell-type specific and mitochondria targeting molecular approach for mitochondrial Ca^{2+} imaging in astrocytes and neurons *in vitro* and *in vivo*. We constructed DNA plasmids encoding mitochondria-targeting genetically encoded Ca^{2+} indicators (GECIs) GCaMP5G or GCaMP6s (GCaMP5G/6s) with astrocyte- and neuron-specific promoters gfaABC1D and CaMKII and mitochondria-targeting sequence (mito-). For *in vitro* mitochondrial Ca^{2+} imaging, the plasmids were transfected in cultured astrocytes and neurons to express GCaMP5G/6s. For *in vivo* mitochondrial Ca^{2+} imaging, adeno-associated viral vectors (AAVs) were prepared and injected into the mouse brains to express GCaMP5G/6s in mitochondria in astrocytes and neurons. Our approach provides a useful mean to image mitochondrial Ca^{2+} dynamics in astrocytes and neurons to study the relationship between cytosolic and mitochondrial Ca^{2+} signaling, as well as astrocyte-neuron interactions.

Introduction

Mitochondria are dynamic subcellular organelles and are considered as the cell powerhouses for energy production. On the other hand, mitochondria can take up Ca^{2+} in the matrix in response to local or cytosolic Ca^{2+} rises. Mitochondrial Ca^{2+} uptake affects mitochondrial function, including metabolic processes such as reactions in the tricarboxylic acid (TCA) cycle and oxidative phosphorylation, and regulates Ca^{2+}-sensitive proteins under physiological conditions[1,2,3,4]. Mitochondrial Ca^{2+} overloading is also a determinant for

Corresponding Author: Shinghua Ding, dings@missouri.edu.

A complete version of this article that includes the video component is available at http://dx.doi.org/10.3791/62917.

Disclosures

The authors have nothing to disclose.

cell death, including necrosis and apoptosis in various brain disorders[5,6,7]. It causes the opening of mitochondrial permeability transition pores (mPTPs) and the release of caspase cofactor, which initiate apoptotic cell death. Therefore, it is important to study mitochondrial Ca^{2+} dynamics and handling in living cells to understand cellular physiology and pathology better.

Mitochondria maintain matrix Ca^{2+} homeostasis through a balance between Ca^{2+} uptake and efflux. Mitochondrial Ca^{2+} uptake is mainly mediated by mitochondrial Ca^{2+} uniporters (MCUs), while mitochondrial Ca^{2+} efflux is mediated by the Na^{+}-Ca^{2+}-Li^{+} exchangers (NCLXs) and the H^{+}/Ca^{2+} exchangers (mHCXs)[8]. The balance can be perturbed through the stimulation of G-protein coupled receptors (GPCRs)[9]. Mitochondrial Ca^{2+} homeostasis is also affected by mitochondrial buffering by the formation of insoluble xCa^{2+}-xPO_4x-xOH complexes[8].

Intracellular and mitochondrial changes in Ca^{2+} concentration ($[Ca^{2+}]$) can be evaluated by fluorescent or luminescent Ca^{2+} indicators. Ca^{2+} binding to indicators causes spectral modifications, allowing to recording of free cellular $[Ca^{2+}]$ in real-time in live cells. Two types of probes are currently available to monitor Ca^{2+} changes in cells: organic chemical incdictors and genetically-encoded Ca^{2+} indicators (GECIs). Generally, different variants with different Ca^{2+} affinities (based on K_d), spectral properties (excitation and emission wavelengths), dynamic ranges, and sensitivities are available for the biological questions under investigation. Although many synthetic organic Ca^{2+} indicators have been used for cytosolic Ca^{2+} imaging, only a few can be selectively loaded in the mitochondrial matrix for mitochondrial Ca^{2+} imaging, with Rhod-2 being the most widely used (for reviews see[10,11]). However, Rhod-2 has a major drawback of leakage during long time-course experiments; in addition, it is partitioned between mitochondria, other organelles and the cytosol, making absolute measurements in different subcompartments difficult. In contrast, by using cell-type specific promoters and subcellular compartment targeting sequences, GECIs can be expressed in different cell types and subcellular compartments for cell- and compartment-specific Ca^{2+} imaging *in vitro* or *in vivo*. Single-wavelength fluorescence intensity-based GCaMP Ca^{2+} indicators have recently emerged as major GECIs[12,13,14,15,16]. In this article, we provide a protocol for mitochondria-targeting and cell-type specific expression of GCaMP5G and GCaMP6s (GCaMP5G/6s) in astrocytes and neurons, and imaging mitochondrial Ca^{2+} uptake in astrocytes and neurons. Using this protocol, the expression of GCaMP6G/6s in individual mitochondria can be revealed and Ca^{2+} uptake in single mitochondrial resolution can be achieved in astrocytes and neurons *in vitro* and *in vivo*.

Protocol

Procedures involving animals have been approved by the Institutional Animal Care and Use Committee (IACUC) at the University of Missouri-Columbia.

1. Construction of DNA plasmids

NOTE: For *in vitro* and *in vivo* imaging, DNA plasmid with astrocyte- and neuron-specific promoters encoding GCaMP5G/6s are constructed with mitochondrial targeting sequences.

1. Insert mitochondrial matrix (MM)-targeting sequence (mito-) ATGT CCGTCCTGAC GCCGCTGCTG CTGCGGGGCT TGACAGGCTC GGCCCGGCGG CTCCCAGTGC CGCGCGCCAA GATCCATTCG TTG[17] into the cloning sites EcoRI and BamHI in the backbone of adeno-associated virus (AAV) plasmid pZac2.1 to obtain plasmids containing astrocytic gfaABC$_1$D promoter or neuronal CaMKII promoter[18,19,20].

2. Subclone GCaMP5G/6s into the cloning sites BamH I and Not 1 in the above plasmids to obtain new plasmids pZac-gfaABC1D-mito-GCaMP5G/6s and pZac-CaMKII-mito-GCaMP5G/6s that target transgene expression in mitochondria in astrocytes and neurons[20,21] (Figure 1A).

3. Prepare pZac-gfaABC1D-mito-GCaMP5G and pZac-CaMKII-mito-GCaMP6s DNA plasmids for transfection for *in vitro* study (Section 2). Produce AAV vectors with serotype 5 for astrocytes and serotype 9 for neurons for *in vivo* study[18] (Section 3).

2. *In vitro* mitochondrial Ca^{2+} imaging in astrocytes and neurons

1. Prepare primary astrocytes from the cortex of P1 neonatal mice and primary neurons from the cortex of E15–16 embryos[18,22,23,24,] and culture them on 12 mm diameter glass coverslips in 24-well plates using Dulbecco's Modified Eagle Medium (DMEM) containing 10% fetal bovine serum (FBS), and neuronal basal medium (NBM) containing 2% B27, respectively.

2. Transfect mature astrocytes and neurons with pZac-gfaABC1D-GCaMP6s and pZac-CaMKII-GCaMP5G plasmids using lipid based transfection reagent to express GCaMP6s in the mitochondria of astrocytes and GCaMP5G in the mitochondria of neurons[18,20,21]. Transfect cells in each well with 0.5 μg of DNA, and change the medium 6 h later.

   NOTE: The astrocytes and neurons are ready for imaging 1–2 days after transfection.

3. Perform *in vitro* mitochondrial Ca^{2+} imaging 1–2 days after transfection.

   1. Transfer the glass coverslips cultured with astrocytes or neurons to the PH-1 perfusion chamber under an epifuorescence or two photon microscope.

   2. Stimulate astrocytic mitochondrial Ca^{2+} uptake with 100 μM ATP in ACSF, or stimulate neuronal mitochondria with 100 μM glutamate/10 μM glycine[20,25] (Figure 2 and Figure 3).

      NOTE: Solution changes from ACSF to ATP- and glutamate/glycine-containing ACSF are controlled by an ALA-VM8 perfusion system[21]. The speed of the solution change is controlled at 1–2 mL/min by adjusting a valve.

3. *In vivo* mitochondrial Ca^{2+} imaging in astrocytes and neurons

1. AAV preparations.
    1. Prepare the following recombinant adeno-associated virus (rAAV) vectors using the DNA plasmids prepared in section 1: rAAV2/5-gfaABC1D-mito-GCaMP5G and rAAV2/9-CaMKII-mito-GCaMP6s vectors.

        NOTE: In this experiment, rAAV vectors of serotype 5 were prepared to express GCaMP5G in mitochondria in astrocytes and rAAV vectors of serotype 9 were prepared to express GCaMP6s in mitochondria for neurons.
2. Stereotaxic AAV injection.
    1. Anesthetize the mouse with 3% isoflurane.

        NOTE: Later during the surgery, the isoflurane levels are reduced to 2%.
    2. After the mouse reaches a surgical level of anesthesia, as determined by tail and toe pinch, shave the hair over the surgery site, motor or somantosensory cortex, with a hair trimmer.
    3. Position the mouse on the mouse stereotaxic device and fix the head with ear bars. Apply ophthalmic ointment to the eyes to protect them during the surgery. Use a heating pad to keep the body temperature of the mouse at 37 °C throughout the surgery.

        NOTE: Perform surgery using aseptic procedures. All surgical tools need to be sterilized either by autoclaving or using a hot bead sterilizer.
    4. After the mouse is mounted on the stereotaxic device, sterilize the scalp with alternating iodine based scrub and 70% ethanol three times. Make an incision in the midline of the scalp to expose the injection site.
    5. Cut open the skin in the bregma lamda axis and a create a ~1 mm diameter burr hole with a high speed drill at the intended injection location of motor or somantosensory cortex.
    6. Use a 33 G Hamilton syringe containing associated adenovirus (rAAV2/5-gfaABC1D-mito-GCaMP5G vectors [1×10^{11} GC] and rAAV2/9-CaMKII-mito-GCaMP6s vectors [1×10^{11} GC]) into the walls of mouse target area to inject upto 1 μL of vectors at the target area.

        NOTE: For example, for cortical viral delivery, inject the virus solution at two depths in multiple steps. First insert the needle upto 1 mm depth and allow 5 min for the brain to recover. Then, move the needle up to ~700 μm depth and inject 500 nL of the virus solution at an injection speed of 10 nL/s using a hamilton syringe controlled by a microsyringe pump controller. After the injection is completed, wait for 5 min to

allow the virus to diffuse into the brain. Then, move the needle up to the second injection location upto a depth of 300 μm. Here, inject an additional 500 nL of the virus solution. Wait for 10 min to allow th virus to diffuse into the brain.

7. Close the scalp and the skin using a tissue adhesive. Let the mice recover on the heating pad. Send mice back to the animal facility after recovery.

3. Cranial-window intstallation and *in vivo* 2-P imaging of mitochondrial Ca^{2+} signals.

NOTE: Cranial window implantation is done 3 weeks post AAV injection over the motor or somatosensory cortex[26,27,28,29]. Subcutanous injection of carprofen (10 mg/Kg) is injected to provide relief from potential pain before surgery. The cranial window surgical procedures are identical to the AAV injection surgical procedures and are performed under aseptic conditions.

1. Anesthetize the mouse with 3% isoflurane.

   NOTE: This is the initial dose and reduce to 2% for the surgery later on. During imaging, an intraperitoneal (IP) injection of 130 mg ketamine/10 mg xylazine/kg body weight dissolved in ACSF during imaging.

2. Position the mouse on the mouse stereotaxic device and fix the head with ear bars. Apply ophthalmic ointment to eyes. Use a heating pad to keep the body temperature of the mouse at 37 °C throughout the surgery.

   NOTE: All surgical tools need to be sterilized.

3. Make an incision of 5–8 mm long in the midline of the scalp and remove a flap of skin using a pair of scissors.

4. After skull is exposed, perform 2.0–3.0 mm diameter crianiotomy using a high-speed drill over the virus injected area (i.e., motor cortex or somatosensory cortex, Figure 1B). First make four small holes, and then drill along in a circle connecting the holes. Then, lift the bone with sharp scissors and remove. The exposed duramater can be removed or kept intact for impantation of the cranial window.

5. Place a glass coverslip of 3–5 mm in diameter carrying a transparent silicone over the craniotomy. Use a toothpick to push the cranial window gently onto the surface of the brain. Then, seal the edge with a small amount of silicone adhesive.

   NOTES: Alternatively, instead of silicone disk, 1.2% low melting point agarose gel can be used between the cover glass and the brain tissue.

6. Finally, seal the edges of the coverslip with dental cement. Take care to apply the cement slightly at the edge of the dental window for strong

bonding. Attach a custom-made metal head plate to the skull with cyanocrylate glue.

NOTE: The metal plate is used to fix the head of the mouse to the stage of 2-P microscope during the imaging session (Figure 1C).

7. Add 0.5 mL of ACSF solution over the coverslip on the cranial window.

8. Perform time-lapse *in vivo* 2-P imaging of mito-GCaMP5G in astrocyte and mito-GCaMP6s in neurons with 910 nm wavelength through the cranial window (Figure 1C)[18,20,27].

   NOTE: During imaging, mice are on the heating pad to maintain physiological temperature. The mice will be sacrificed immediately after the imaging session is completed.

9. Label astrocytes *in vivo* with sulforhodamine 101 (SR101) when it is necessary to determine colocaliztion.

   1. At end of step 3.3.4, apply 100 μL of 100 μM SR101 in ACSF on the cortical surface for 1–5 min.

   2. Rinse the surface with ACSF to wash away the unbound SR101. Using 2-P imaging, co-labeling of mito-GCaMP5G and SR101 in astrocytes can be observed 45–60 min later (Figure 4A).

Representative Results

The aim of this study was to provide methodology to image mitochondrial Ca^{2+} signal using GECIs in astrocytes and neurons *in vitro* and *in vivo*. Results of both *in vitro* and *in vivo* mitochondrial ca^{2+} imaging are presented here.

In vitro mitochondrial Ca^{2+} signaling in cultured astrocytes and neurons

Mitochondrial Ca^{2+} uptake in astrocytes can be elicited by ATP application, and mitochondrial Ca^{2+} uptake in neurons can be elicited by glutamate and glycine application through a perfusion system. Figure 2 and Figure 3 show GCaMP6s is expressed in cultured astrocytes and GCaMP5G in neurons, respectively. Mitochondrial Ca^{2+} uptake in astrocytes was elicited by 100 μM ATP with individual mitochondrial resolution (Figure 2B–D). Mitochondrial Ca^{2+} uptakes in neurons was elicited by 100 μM glutamate and 10 μM glycine with individual mitochondrial resolution (Figure 3B–D).

In vivo 2-P imaging of mitochondrial expression of GCaMP5G or 6S in astrocytes and neurons

The imaging is done by collecting time-lapse *in vivo* 2-P imaging of mitochondrial fluorescence signals in astrocytes and neurons with an Ultima 2-P microscope system. We use exciation wavelength 880–910 nm. Figure 4 shows expression of GCaMP5G in mitochondria in astrocytes in the mouse cortex. The astrocyte-specific expression of GCaMP5G was confirmed by colocalization of SR101 with GCaMP5G with individual

mitochondria resolution (Figure 4A), and spontaneous Ca^{2+} changes in individual mitochondria can be observed (Figure 4B–E). Figure 5A shows neuron-specific expression of mito-GCaMP6s colocalized with neuronal marker NeuN. The fluorescence of mito-GCaMP6s in neurons shows mitochondrial morphology in dendrites (Figure 5B). Spontaneous mitochondrial Ca^{2+} increases in dendrites can be observed (Figure 5C–F).

Analysis of mitochondrial Ca^{2+} signals

Quantify the fluorescent signals by calculating the mean pixel intensities of the cell body or individual mitochondria in astrocytes and neurons using image analysis software. Ca^{2+} changes overtime (t) are expressed as F/Fo (t) values versus time, where Fo is the background subtracted baseline fluorescence and F is the baseline subtracted fluorescence change[20,21]. Use the peak F/Fo values to compare the amplitude of Ca^{2+} signals.

Discussion

In this article, we provide a method and protocol for imaging mitochondrial Ca^{2+} in astrocytes and neurons. We implemented mitochondria-targeting and cell type-specific strategies to express GECI GCaMP5G/6s. To target GCaMP5G/6s in mitochondria, we included a mitochondria-targeting sequence in the plasmids. To express GCaMP5G/6s in astrocytes and neurons *in vivo*, we inserted an astrocyte-specific promoter gfaABC1D and neuron-specific promoter CaMKII into the plasmids. Cell-type specific expression of GCaMP5G/6s in astrocytes and neurons can be confirmed by SR101 labeling in astrocytes and immunostaining of neurons with NeuN. From our data, these strategies provide a reliable cell type specific approach for mitochondrial Ca^{2+} imaging in astrocytes and neurons *in vivo*.

One potential problem for GECI expression is that it might cause Ca^{2+} buffering since it may reduce free Ca^{2+} by Ca^{2+} binding. Another problem that might be paid attention to is the amount of virus injected. Individual cells expressing GECI may not be identified if excessive virus is injected. These problems can be effectively ameliorated by reducing the titer of AAV. Photobleaching might also be an issue. Theoretically, all fluorescent indicators are subject to photobleaching. GCaMP5G/6s are quite stable, but they will bleach under continual exposure to excitation light. One general practice to avoid photobleaching is to reduce exposure time of tissue to laser light while ensuring enough fluorescence is collected. This can be achieved if high sensitivity PMTs and high light transmission objective are used. Photobleaching can also be reduced by closing shutter between images.

In our results of *in vivo* 2-P imaging, spontaneous mitochondrial increases can be observed both in astrocyte and neurons. Notably, these mitochondrial Ca^{2+} transients have long durations (Figure 4E and Figure 5E), consistent with a recent report by Gobel et al.[30]. The underlying mechanism of this phenomenon is not clear but is worth being pursued further. For cytosolic Ca^{2+} increase, astrocytes and neurons have different mechanisms. G-protein receptor stimulations cause Ca^{2+} increase in ER in astrocytes while the activations of voltage gated Ca^{2+} channels or glutamate receptors cause cytosolic Ca^{2+} increase in neurons, which can be uptaken by mitochondria. In our previous study[20], we found that when mito-GCaMP5G was cotransfected with IP_3 5-phosphatase (5ppase) cultured astrocytes,

ATP-induced mitochondrial Ca^{2+} increase could be largely abolished. However, the two mutants of 5ppase, i.e., R343A and R343A/R350A 5ppase, which lack enzymatic activity, did not affect the mitochondrial Ca^{2+} increase after ATP stimulation. The results indicate that cytosolic and mitochondrial Ca^{2+} levels are highly coupled, likely because of the intimate physical connection between the ER and mitochondria in astrocytes, with the cytosol serving as an intermediary conduit for Ca^{2+} delivery. We also found that glutamate stimulation caused mitochondrial Ca^{2+} increase in neurons, suggesting glutamate receptors play a role in Ca^{2+} entry from extracellular space. In the future, it will be interesting to study sensory-driven mitochondrial Ca^{2+} increases in astrocytes and neurons.

Our approach can be used to simultaneously image cytosolic and mitochondrial Ca^{2+} signals in the same cell type when two GECIs of different fluorescence wavelengths are expressed simultaneously, e.g., a red florescence GECI RCaMP in cytoplasm and GCaMP in mitochondria, or vice versa[31]. This approach can also be used for the *in vivo* study of astrocyte-neuron interactions in physiology and pathology with GCaMP expressed in astrocytes and RCaMP in neurons, or vice versa.

GCaMP is a GFP-based single fluorophore GECI. Currently, GCaMPs are the most preferred Ca^{2+} indicators because of their high signal-to-noise ratio (SNR), and large dynamic ranges (DR). Recently, jGCaMP7 sensors, the optimized version of GCaMP6, were reported with improved sensitivity to individual spikes[16]. GCaMP7 sensors can be easily subcloned in our plasmids for mitochondrial Ca^{2+} imaging. In summary, the strategies we presented here can be used to image mitochondrial Ca^{2+} uptake and handling in neurons and astrocytes with sufficient sensitivity to resolve Ca^{2+} changes at single mitochondrial level *in vivo*. This protocol represents a useful means to study cytosolic and mitochondrial Ca^{2+} signaling in astrocytes and neurons, as well as astrocyte-neuron interactions.

Acknowledgments

This work was supported by the National Institute of Health National Institute of Neurological Disorders and Stroke (NINDS) grants R01NS069726 and R01NS094539 to SD. We thank Erica DeMers for audio recording.

References

1. Griffiths EJ, Rutter GA Mitochondrial calcium as a key regulator of mitochondrial ATP production in mammalian cells. Biochimica et Biophysica Acta (BBA) - Bioenergetics. 1787 (11), 1324–1333 (2009). [PubMed: 19366607]
2. Pizzo P, Drago I, Filadi R, Pozzan T Mitochondrial Ca^{2+} homeostasis: mechanism, role, and tissue specificities. Pflugers Archiv - European Journal of Physiology. 464 (1), 3–17 (2012). [PubMed: 22706634]
3. Llorente-Folch I et al. Calcium-regulation of mitochondrial respiration maintains ATP homeostasis and requires ARALAR/AGC1-malate aspartate shuttle in intact cortical neurons. The Journal of Neuroscience. 33(35), 13957–13971 (2013). [PubMed: 23986233]
4. Burkeen JF, Womac AD, Earnest DJ, Zoran MJ Mitochondrial calcium signaling mediates rhythmic extracellular ATP accumulation in suprachiasmatic nucleus astrocytes. The Journal of Neuroscience. 31(23), 8432–8440 (2011). [PubMed: 21653847]
5. Duchen M Mitochondria, calcium-dependent neuronal death and neurodegenerative disease. Pflugers Archiv - European Journal of Physiology. 464 (1), 111–121 (2012). [PubMed: 22615071]
6. Gouriou Y, Demaurex N, Bijlenga P, De Marchi U Mitochondrial calcium handling during ischemia-induced cell death in neurons. Biochimie. 93 (12), 2060–2067 (2011). [PubMed: 21846486]

7. Qiu J et al. Mitochondrial calcium uniporter Mcu controls excitotoxicity and is transcriptionally repressed by neuroprotective nuclear calcium signals. Nature Communications. 4, 2034 (2013).
8. Filadi R, Greotti E The yin and yang of mitochondrial Ca^{2+} signaling in cell physiology and pathology. Cell Calcium. 93, 102321 (2021). [PubMed: 33310302]
9. Finkel T et al. The ins and outs of mitochondrial calcium. Circulation Research. 116 (11), 1810–1819 (2015). [PubMed: 25999421]
10. Paredes RM, Etzler JC, Watts LT, Zheng W, Lechleiter JD Chemical calcium indicators. Methods. 46 (3), 143–151 (2008). [PubMed: 18929663]
11. Contreras L, Drago I, Zampese E, Pozzan T Mitochondria: The calcium connection. Biochimica et Biophysica Acta (BBA). 1797 (6–7), 607–618 (2010). [PubMed: 20470749]
12. Tian L et al. Imaging neural activity in worms, flies and mice with improved GCaMP calcium indicators. Nature Methods. 6 (12), 875–881 (2009). [PubMed: 19898485]
13. Yamada Y et al. Quantitative comparison of genetically encoded Ca^{2+} indicators in cortical pyramidal cells and cerebellar Purkinje cells. Frontiers in Cellular Neuroscience. 5, 18 (2011). [PubMed: 21994490]
14. Akerboom J et al. Optimization of a GCaMP Calcium Indicator for Neural Activity Imaging. The Journal of Neuroscience. 32 (40), 13819–13840 (2012). [PubMed: 23035093]
15. Chen TW et al. Ultrasensitive fluorescent proteins for imaging neuronal activity. Nature. 499 (7458), 295–300 (2013). [PubMed: 23868258]
16. Dana H et al. High-performance calcium sensors for imaging activity in neuronal populations and microcompartments. Nature Methods. 16 (7), 649–657 (2019). [PubMed: 31209382]
17. Rizzuto R, Brini M, Pizzo P, Murgia M, Pozzan T Chimeric green fluorescent protein as a tool for visualizing subcellular organelles in living cells. Current Biology: CB. 5 (6), 635–642 (1995). [PubMed: 7552174]
18. Xie Y, Wang T, Sun GY, Ding S Specific disruption of astrocytic Ca^{2+} signaling pathway in vivo by adeno-associated viral transduction. Neuroscience. 170 (4), 992–1003 (2010). [PubMed: 20736051]
19. Lee Y et al. GFAP promoter elements required for region-specific and astrocyte-specific expression. Glia. 56 (5), 481–493 (2008). [PubMed: 18240313]
20. Li H et al. Imaging of mitochondrial Ca^{2+} dynamics in astrocytes using cell-specific mitochondria-targeted GCaMP5G/6s: Mitochondrial Ca^{2+} uptake and cytosolic Ca^{2+} availability via the endoplasmic reticulum store. Cell Calcium. 56 (6), 457–466 (2014). [PubMed: 25443655]
21. Zhang N, Ding S Imaging of mitochondrial and cytosolic Ca^{2+} signals in cultured astrocytes. Current Protocols in Neuroscience. 82, 2.29.1–2.29.11 (2018). [PubMed: 29357111]
22. Bi J, Li H, Ye SQ, Ding S Pre-B-cell colony-enhancing factor exerts a neuronal protection through its enzymatic activity and the reduction of mitochondrial dysfunction in in vitro ischemic models. Journal of Neurochemistry. 120 (2), 334–346 (2012). [PubMed: 22044451]
23. Wang X, Li H, Ding S Pre-B-cell colony-enhancing factor protects against apoptotic neuronal death and mitochondrial damage in ischemia. Scientific Reports. 6, 32416 (2016). [PubMed: 27576732]
24. Wang X et al. Subcellular NAMPT-mediated NAD^{+} salvage pathways and their roles in bioenergetics and neuronal protection after ischemic injury. Journal of Neurochemistry. 151 (6), 732–748 (2019). [PubMed: 31553812]
25. Xie Y, Chen S, Wu Y, Murphy TH Prolonged deficits in parvalbumin neuron stimulation-evoked network activity despite recovery of dendritic structure and excitability in the somatosensory cortex following global ischemia in mice. The Journal of Neuroscience. 34 (45), 14890–14900 (2014). [PubMed: 25378156]
26. Ding S In vivo imaging of Ca^{2+} signaling in astrocytes using two-photon laser scanning fluorescent microscopy in *Astrocytes*. (ed. Milner R) Humana Press. 545–554 (2012).
27. Li H et al. Disruption of IP_3R2-mediated Ca^{2+} signaling pathway in astrocytes ameliorates neuronal death and brain damage while reducing behavioral deficits after focal ischemic stroke. Cell Calcium. 58 (6), 565–576 (2015). [PubMed: 26433454]
28. Ding S et al. Photothrombosis ischemia stimulates a sustained astrocytic Ca^{2+} signaling in vivo. Glia. 57 (7), 767–776 (2009). [PubMed: 18985731]

29. Ding S et al. Enhanced astrocytic Ca^{2+} signals contribute to neuronal excitotoxicity after status epilepticus. The Journal of Neuroscience. 27 (40), 10674–10684 (2007). [PubMed: 17913901]

30. Gobel J et al. Mitochondria-endoplasmic reticulum contacts in reactive astrocytes promote vascular remodeling. Cell Metabolism. 31 (4), 791–808 (2020). [PubMed: 32220306]

31. Diaz-Garcia CM et al. The distinct roles of calcium in rapid control of neuronal glycolysis and the tricarboxylic acid cycle. eLife. 10, e64821 (2021). [PubMed: 33555254]

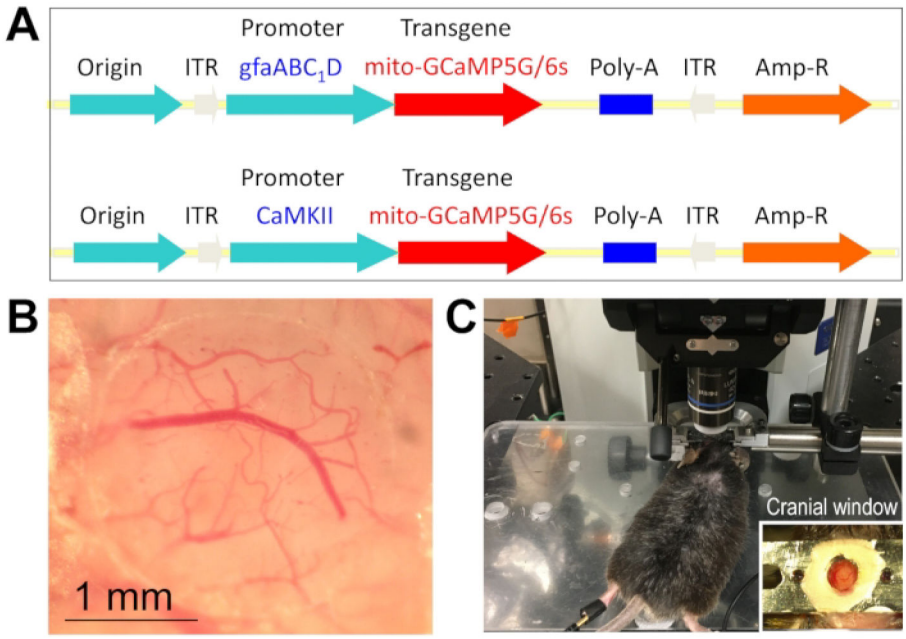

Figure 1: DNA constructs for astrocyte- and neuron-specific and mitochondria-targeting transgene expression, and *in vivo* 2-P imaging.

(**A**) DNA Constructs of genetically encoded Ca^{2+} indicator GCaMP5G or GcaMP6s in pZac2.1 plasmid with gfaABC$_1$D (up) and CaMKII (low) promoters for delivery to astrocytic and neuronal mitochondrial matrix, respectively. Mitochondria-targeting is achieved using a mitochondrial matrix (MM) specific sequence (mito) appended to the N-terminus of the fluorescent proteins. (**B**) A craniotomy over the cortex of a mouse. (**C**) The skull of a mouse is attached to a metal plate connected to the post fixed on the stage of 2-P microscope. The inset shows the cranial window with a metal plate attached to the skull.

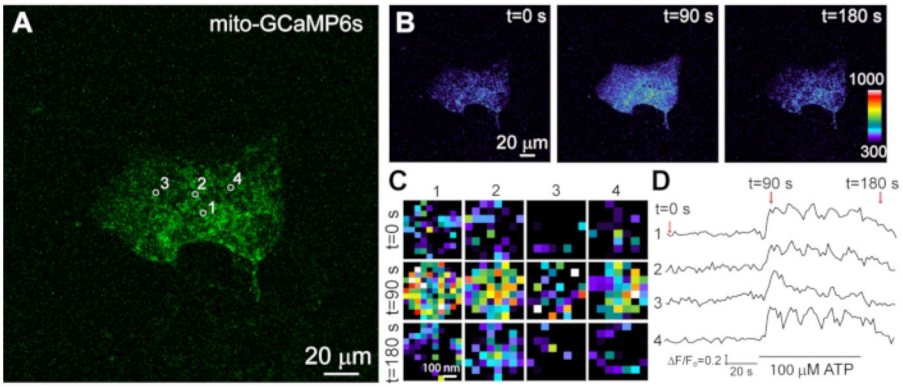

Figure 2: Mitochondrial Ca^{2+} imaging of cultured astrocytes.

(**A-B**) A 2-P image of an astrocyte expressing mito-GCaMP6s (**A**) and its response to the stimulation of 100 μM ATP at the indicated time (**B**). (**C**) Images of mito-GCaMP6sin the four individual mitochondria (in A, circles) at the different times after ATP stimulation. (**D**) The time courses of mito-GCaMP6s fluorescence changes, plotted as ΔF/Fo, in the four individual mitochondria after ATP stimulation. The red arrow indicates the starting time of imaging. The pseudocolor scale is a linear representation of the fluorescence intensity in this and other figures.

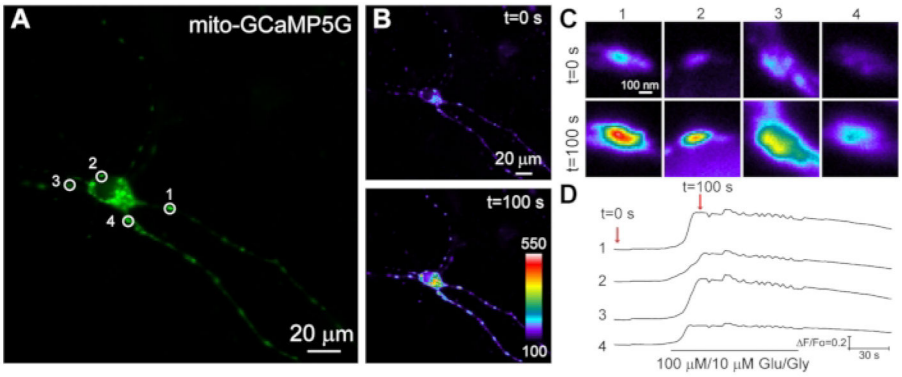

Figure 3: Mitochondrial Ca^{2+} imaging of cultured neurons.

(**A-B**) A 2-P images of mito-GCaMP5G expressingneuron (**A**) and its response to 100 μM glutamate at the indicated times (**B**). (**C**) Images of mito-GCaMP5G in the four individual mitochondria (in A, circles) at different times after glutamate stimulation. (**D**) The time courses of mito-GCaMP5G fluorescence changes in the four individual mitochondria.

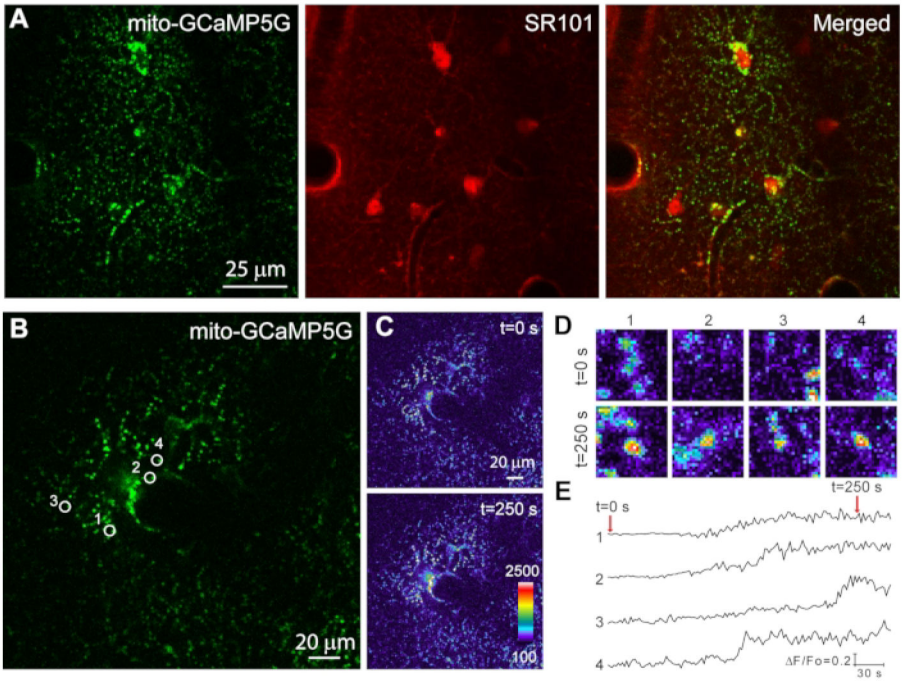

Figure 4: *In vivo* 2-P imaging of mitochondrial Ca^{2+} signaling in astrocytes.

(**A**) 2-P images of mito-GCaMP5G expressing astrocytes colocalized with SR101. (**B-C**) 2-P image of an astrocyte expressing mito-GCaMP5G for analysisof spontaneous Ca^{2+} increase. (**C-E**) Images of mito-GCaMP5G in the four individual mitochondria in the astrocyte (in B, circles) at the different times (C) and the time courses of mito-GCaMP5G fluorescence changes, plotted as ΔF/Fo, in the four individual mitochondria (E).

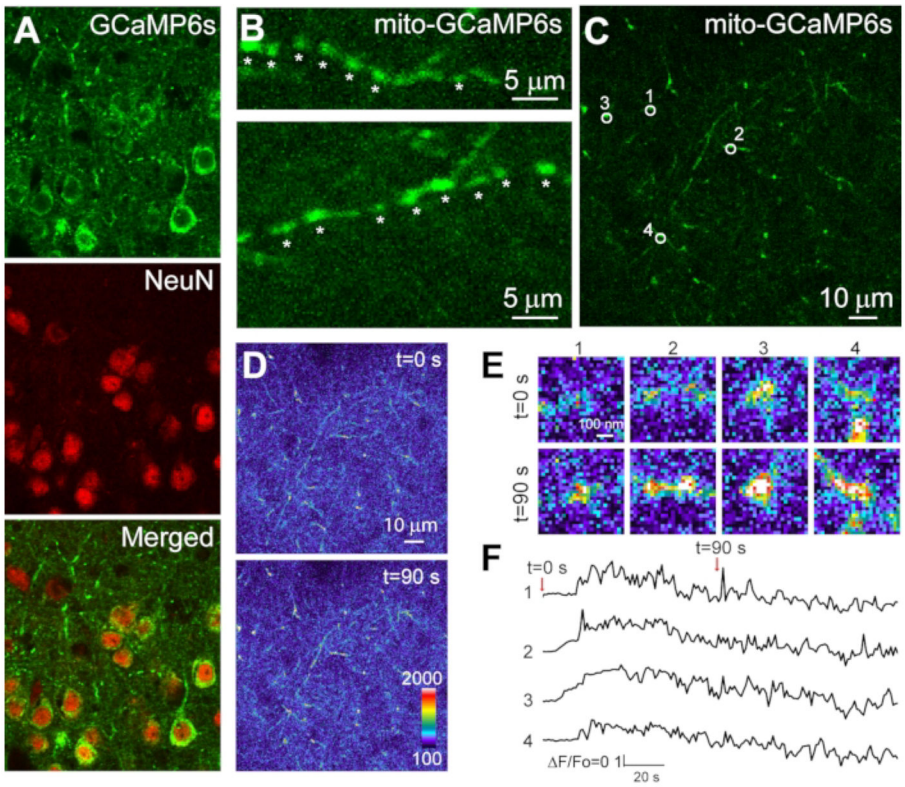

Figure 5: *In vivo* 2-P imaging of mitochondrial Ca^{2+} signaling in neurons.

(**A**) Colocalization of GCaMP6s (upper) with neuronal marker NeuN (middle) in the brain. (**B**) High resolution images of dendrites expressing GCaMP6s with mitochondrial morphology (indicated by *s). (**C**) GCaMP6s expressed in neuronal mitochondria. (**D-F**) Analysis of spontaneous mitochondrial Ca^{2+} increase in neurons. Pseudocolor 2-P image of the mitochondria expressing mito-GCaMP6s in C at different times (**D**). Images of mito-GCaMP6s in the four individual mitochondria in C (circles) at the different times (**E-F**) and the time courses of mito-GCaMP6s fluorescence changes, plotted as ΔF/Fo, in the four individual mitochondria (**F**).

Movie:

Mitochondrial Ca^{2+} increases based on GCaMP5G fluorescence changes in response to 100 μM ATP in cultured astrocytes.